Neuro-Oncology 13(3):280–289, 2011.
doi:10.1093/neuonc/noq190

DNA hypermethylation profiles associated with glioma subtypes and EZH2 and IGFBP2 mRNA expression

Shichun Zheng, E. Andres Houseman, Zachary Morrison, Margaret R. Wrensch, Joseph S. Patoka, Christian Ramos, Daphne A. Haas-Kogan, Sean McBride, Carmen J. Marsit, Brock C. Christensen, Heather H. Nelson, David Stokoe, Joseph L. Wiemels, Susan M. Chang, Michael D. Prados, Tarik Tihan, Scott R. Vandenberg, Karl T. Kelsey, Mitchel S. Berger, and John K. Wiencke

Departments of Neurological Surgery, Epidemiology, and Biostatistics and Pathology, University of California San Francisco, San Francisco, California (S.Z., Z.M., M.R.W., J.S.P., C.R., D.A.H., S.M., J.L.W., S.M.C., M.D.P., T.T., S.R.V., M.S.B., J.K.W.); Departments of Community Health and Pathology and Laboratory Medicine, Brown University, Providence, Rhode Island (E.A.H., C.J.M., B.C.C., K.T.K.); Genentech Inc., South San Francisco, California (D.S.); Masonic Cancer Center, Division of Epidemiology and Community Health, University of Minnesota, Minneapolis, Minnesota (H.H.N.)

We explored the associations of aberrant DNA methylation patterns in 12 candidate genes with adult glioma subtype, patient survival, and gene expression of enhancer of zeste human homolog 2 (*EZH2*) and insulin-like growth factor-binding protein 2 (*IGFBP2*). We analyzed 154 primary glioma tumors (37 astrocytoma II and III, 52 primary glioblastoma multiforme (GBM), 11 secondary GBM, 54 oligodendroglioma/oligoastrocytoma II and III) and 13 nonmalignant brain tissues for aberrant methylation with quantitative methylation-specific PCR (qMS-PCR) and for *EZH2* and *IGFBP2* expression with quantitative reverse transcription PCR (qRT-PCR). Global methylation was assessed by measuring long interspersed nuclear element-1 (LINE1) methylation. Unsupervised clustering analyses yielded 3 methylation patterns (classes). Class 1 (*MGMT, PTEN, RASSF1A, TMS1, ZNF342, EMP3, SOCS1, RFX1*) was highly methylated in 82% (75/91) of lower-grade astrocytic and oligodendroglial tumors, 73% (8/11) of secondary GBMs, and 12% (6/52) of primary GBMs. The primary GBMs in this class were early onset (median age 37 years). Class 2 (*HOXA9* and *SLIT2*) was highly methylated in 37% (19/52) of primary GBMs. None of the 10 genes for class 3 that were differentially methylated in classes 1 and 2 were hypermethylated in 92% (12/13) of nonmalignant brain tissues and 52% (27/52) of primary GBMs. Class 1 tumors had elevated *EZH2* expression but not elevated *IGFBP2*; class 2 tumors had both high *IGFBP2* and high *EZH2* expressions. The gene-specific hypermethylation class correlated with higher levels of global LINE1 methylation and longer patient survival times. These findings indicate a generalized hypermethylation phenotype in glioma linked to improved survival and low IGFBP2. DNA methylation markers are useful in characterizing distinct glioma subtypes and may hold promise for clinical applications.

Keywords: glioma, DNA methylation, EZH2, Polycomb, PI3K/Akt.

Human gliomas are histologically and molecularly heterogeneous CNS malignancies.[1] These marked differences in histological as well as epidemiologic characteristics[2,3] of glioma have prompted many studies that have revealed genetic[4] and gene expression patterns that characterize different glioma subgroups. Less numerous are studies of epigenetic abnormalities, although such alterations, including aberrant DNA methylation of putative tumor-suppressor genes (TSGs), are powerful markers for classifying human cancer.[5] We and others studying individual TSGs found hypermethylation to be more common among secondary glioblastoma multiformes (GBMs)

Received November 10, 2009; accepted September 9, 2010.

Corresponding Author: John K. Wiencke, Department of Neurological Surgery, University of California–San Francisco, Helen Diller Family Cancer Center, 1450 3rd Street, San Francisco, CA 94158 (John.Wiencke@ucsf.edu).

than among primary GBMs.[6–10] Other groups have reported coordinate methylation of multiple genes in glioma and have suggested that DNA methylation is associated with tumor grade.[11–13] Given these observations, we hypothesized that different patterns of DNA methylation could delineate secondary from primary GBM and differentiate GBM (grade IV) from lower-grade gliomas. We examined a limited number of genes based on previous studies indicating significant alterations in DNA methylation status of the gene in human brain tumors: *MGMT*,[14] *PTEN*,[10] *RASSF1A*,[15] *RFX1*,[16] *EMP3*,[6,17] *TMS1*,[18] *ZNF342*,[19] *SOCS1*,[20] *PEG3*,[21] *MAGEA1*,[22] *HOXA9*,[23] and *SLIT2*.[24] Furthermore, we examined whether overexpression of specific oncogenes might be associated with aberrant DNA methylation to gain mechanistic insight into the epigenetic dysregulation of brain tumors.

The mechanisms responsible for hypermethylation of groups of genes in specific types of human cancers are obscure. Recently, attention has focused on the involvement of Polycomb repressive complexes (PRCs) in DNA methylation and particularly the enhancer of zeste human homolog 2 gene (*EZH2*),[25] which is the catalytic component of the PRC2 and PRC3 complexes.[26] *EZH2* has been shown to control DNA methylation through its ability to produce the nucleosomal histone H3 lysine 27 trimethylation mark (H3K27me3) that provides a platform for recruiting DNA methyltransferases.[27] PRC activation is linked to cell type–specific patterns of gene repression and DNA methylation through the H3K27me3 markings that are produced in stem cells.[26] Thus, PRC gene targets in cancer progenitor cells may be preprogrammed for DNA hypermethylation that is triggered later during cell transformation.[28–30] *EZH2* overexpression is associated with aggressive clinical behavior in prostate, breast, and bladder cancers.[31–37] The suppression of 14 genes that are direct PRC targets in embryonic stem cells defined a gene expression signature that was significantly associated with poor clinical outcome in multiple microarray data sets of tumors, including breast and prostate cancers.[38] Although there have been no investigations of *EZH2* in relationship to DNA methylation in glioma, *EZH2* overexpression has been correlated with hypermethylation of *APAF-1* in bladder cancer[39] and *PSP94* methylation in prostate cancer.[40]

An additional pathway we consider here is the PI3K/Akt pathway, because *EZH2* has been shown to be a target of Akt phosphorylation, and the affinity of EZH2 toward histone H3 and related synthesis of H3K27me3 is greatly reduced in cells with activated Akt.[41] Given the potential importance of H3K27me3 in controlling DNA methylation, we hypothesized that modification of *EZH2* by Akt activation could affect DNA methylation profiles. We chose to use mRNA levels of the insulin-like growth factor-binding protein 2 gene (*IGFBP2*) as a biomarker of PI3K/Akt pathway activation on the basis of studies showing that elevated *IGFBP2* is tightly linked to loss of the phosphatase and tensin homolog gene (*PTEN*) in GBM and that *IGFBP2* may play a functional role in *PTEN*/Akt signaling.[42,43] Supporting this latter notion are observations in murine models of glioma indicating that *IGFBP2* plays a key role in the activation of the Akt pathway.[44] Proteomic studies identified a strong correlation between high concentrations of PI3K, Akt-pThr308, and *IGFBP2* among a 12-protein cluster that distinguished GBM from lower-grade gliomas.[45] In primary human tumors, *IGFBP2* mRNA levels are closely correlated with protein expression of IGFBP2 by Western blot analysis[43] and immunohistochemistry.[46] There is a well-established relationship between high *IGFBP2* expression and increasing glioma tumor grade[47–51] and the presence of necrosis, microvascular proliferation, and shorter survival times.[46,48,49,51]

Materials and Methods

Patients and Tissue Samples

We obtained 154 freshly frozen tumor tissues and 13 samples of nontumor brain from the University of California–San Francisco Brain Tumor Research Center tissue bank under appropriate institutional review board approval. The demographic and tumor characteristics for the glioma patients included in this study are presented in Table 1. Tumor samples were defined as secondary GBM if the patients had prior histological diagnosis of a low-grade glioma. All ages given are at the time of surgery, which occurred at the University of California–San Francisco between 1990 and 2003. Nontumor brain samples are portions of the temporal lobe that were surgically removed as a treatment for epilepsy and processed in the same way as the glioma specimens.

DNA Extraction and Bisulfite Modification

Genomic DNA and RNA were co-isolated from approximately 25 mg wet weight of each frozen tissue

Table 1. Subject Age, Sex, and Histology for Glioma Patients and Controls

Histology/Grade	N	Age, years				Sex	
		Mean	Med	Min	Max	Female (%)	Male (%)
Astrocytoma/II	28	39	38	21	64	11 (39)	17 (61)
Astrocytoma/III	9	42	46	23	61	6 (67)	3 (33)
Primary GBM	52	54	54	22	77	17 (33)	35 (67)
Secondary GBM	11	34	36	15	50	4 (36)	7 (64)
Oligo[a]/II and III	54	39	37	23	60	26 (48)	28 (52)
Nontumor brain	13	36	39	14	52	7 (54)	6 (46)
All	167	42	41	14	77	71 (43)	96 (57)

[a]Oligo includes oligodendroglioma and oligoastrocytoma.

sample using AllPrep DNA/RNA Mini Kit (Qiagen) according to the manufacturer's instructions and eluted twice in a total of 100 μl of elution buffer. This procedure yielded 5–40 μg of genomic DNA. Bisulfite modification of genomic DNA was performed using the EZ DNA Methylation Kit (Zymo Research) according to manufacturer's protocol. CpGenome Universal Methylated DNA (Chemicon International) was chemically converted at the same time and used as a positive control/calibrator.

Quantitative Methylation-Specific PCR for Methylation Analysis

Candidate genes were selected based on previous studies showing their aberrant methylation in astrocytic glioma. See Supplementary Material, Table S1 for primer sequences and the size of amplicon. Because of heterogeneity in *MGMT* methylation, two different regions were targeted. Quantitative methylation-specific real-time PCR was performed on primary tumor samples using the Applied Biosystems 7900HT Fast Real-Time PCR System. The reaction plate was prepared with the Beckman Coulter automated liquid handler–Biomex 3000. Each reaction contained 10.0 μl of 2× Power SYBR Green PCR Master Mix (Applied Biosystems), 100–400 nM of forward and reverse primers, and 2 μl of DNA template in a total volume of 20 μl. For the amplification of *EMP3*, *RASSF1A*, and *RFX1*, 2–3% dimethyl sulfoxide (DMSO) was added. PCR conditions are modified by different primer concentrations, and the addition of DMSO ensured that primer dimers and nonspecific amplification product were not included in the calculation of threshold cycle (Ct). The dissociation curve and agarose gel were run to confirm amplification specificity. All genes were PCR amplified using SYBR Green Real Time PCR Master Mix (Applied Biosystems) under the following conditions: 95° C for 10 min followed by 40 PCR cycles of 95° C 15 s, 60° C for 30 s, and 72° C for 30 s. SYBR green fluorescence data were collected only during the 72° C extension step. Ct values were calculated by the 7900HT system software, and average relative quantification (RQ) values were obtained for each sample, where RQ = (target gene/*ACTB*) / (Universal methylation calibrator/*ACTB*).

Quantitative Reverse Transcription PCR for Gene Expression

We performed quantitative RT-PCR to determine the relative expression levels of *EZH2* and *IGFBP2* on primary tumor samples using a 7900HT Fast Real-Time PCR System (Applied Biosystems). Primers and probes were purchased from Applied Biosystems (ABI) as a premixed gene expression assay for each transcript (see Supplementary Material, Table S1). *EZH2* has two transcriptional variants that encode two distinct proteins; we chose to utilize three assays, two of which would distinguish between each transcript variant and a third that would bind to a common region of both, in order to get a relative quantity for the total *EZH2* expression. Samples were analyzed in triplicate for *EZH2* variant 1, *EZH2* variant 2, total *EZH2*, *IGFBP2*, and *ACTB*, which was used as the endogenous control. All targets were amplified under the following conditions: 95° C for 10 minutes, followed by 40 cycles of 96° C for 15 s, and 60° C for 1 min. All RT-PCR reactions contained a final concentration of 1× Taqman Universal Master Mix, no Amperase UNG (Applied Biosystems, p/n 4324018), 1× of each corresponding Gene Expression Assay reagent, and 3 μl of template cDNA. Relative quantitative expression was determined with Sequence Detection software v2.2.1 (Applied Biosystems) utilizing the delta delta Ct method as previously described.[52] cDNA prepared from normal adult brain RNA (Clontech) was used as the calibrator sample.

EZH2 and EGFR Gene Amplification

Primers for real time-PCR were designed by using Primer Expression version 1.5 software (Applied Biosystems). The housekeeping glyceraldehyde 3-phosphate dehydrogenase gene (*GAPDH*) was used as an internal control for differences in DNA concentration. For each sample, the gene of interest and *GAPDH* were both amplified in triplicate, and results were analyzed by using Sequence Detector version 1.7 and Dissociation Curve version 1.0 software (Applied Biosystems). Relative quantification was performed with the standard curve method, and gene amplification levels were normalized by dividing by *GAPDH* levels in each sample. A cutoff of three copies was considered amplified. Haploid copy numbers were compared by the delta delta Ct method[53] for the mean Ct of the reaction triplicates as follows: $2^{-\Delta\Delta CT} = ((1 + E)^{-\Delta CTgene})/ ((1 + E)^{-\Delta CTreference\ gene})$, where E = efficiency of the PCR reaction (set at default value 0.95), ΔCTgene = difference in Ct value between test sample and calibrator sample (BT71) for the gene under investigation (test gene), and ΔCT reference gene = difference in Ct value between test sample and calibrator sample (BT71) for the reference gene (*GAPDH*). (See Supplementary Material, Table S1 for primer sequence and amplicon size.)

LINE1 Methylation Assay

Global methylation was estimated by measuring long interspersed nuclear element-1 (LINE1) methylation as previously described.[54] Briefly, LINE1 region methylation extent was determined through quantitative bisulfite pyrosequencing. The method examines the cytosine methylation status at 4 cytosine-phosphate-guanine (CpG) sites in the LINE1 region. Each sequencing reaction was run according to instrument manufacturer (Qiagen) protocols on a PyroMarkMD System. Three PCR amplifications were performed on each sample and 2 pyrosequencing runs were done from each PCR, resulting in 6 replicates for each specimen to assess repeat measure variability. The average measure of

LINE1 methylation across the 4 CpG sites was used for each individual tumor.

Statistical Analysis

We used unsupervised learning methods to discover methylation patterns and explore associations with patient characteristics and tumor *EZH2* and *IGFPB2* expression. All analyses were conducted in the R statistical programming environment. We constructed visual representations of raw data using hierarchical clustering with average linkage, applied to pseudo-distances obtained as one minus the Spearman correlation among genes or among the geometric mean methylation for each histology. The resulting image plots were compared with model-based analyses described below. For unsupervised learning, we employed methods that assume discrete classifications (i.e., distinct methylation phenotypes). For discrete clustering, we used the Gaussian mixture model (GMM) framework.[55–58] To address missing values among cases, we used a modified version of the GMM; here, the assumed multivariate Gaussian distribution for each methylation profile i, conditional on a given class, is $N(\mu_i^*, \Sigma_i^*)$, where $N(\mu,\Sigma)$ is the assumed distribution for the fully observed profile, conditional on the given class, and μ_i^*, Σ_i^* are the respective mean vector and covariance matrix obtained by deleting elements of μ and Σ that correspond to missing methylation observations for subject i. Cluster number was selected based on the Bayesian Information Criterion. We compared patient characteristics with methylation classes or propensities using chi-square tests for tabular data or analysis of variance, respectively. In the former case, we used permutation tests or exact methods to protect against possible small cell counts. We compared EZH2 and IGFBP2 expression among tumor classes using two-sample Student's t-tests. Survival follow-up data were available for 103 patients with methylation data. Associations of methylation classification with all-cause patient survival were examined using multivariate Cox proportional hazard models with adjustments for patient age, sex, and tumor grade.

Results

Three Classes of DNA Methylation in Glioma

The characteristics of the study population are presented in Table 1. To visualize the methylation data, we first performed unsupervised hierarchical clustering of samples. Interestingly, most lower-grade astrocytic or oligodendroglial tumors were grouped together with quantitatively higher methylation scores using qMS-PCR. Applying a mixture modeling approach, we next identified 3 classes of DNA methylation among the glioma and normal specimens (Fig. 1). The coordinate methylation of 8 genes (*MGMT*, *PTEN*, *RASSF1A*, *TMS1*, *ZNF342*, *EMP3*, *SOCS1*, and *RFX1*) defined a class of tumors that contained the highest methylation scores compared with the other classes. Among lower-grade tumors, 82% (75/91) fell into this most highly methylated class 1 (Table 2). Only 12% of primary GBMs were classified as class 1 compared with 73% of secondary GBMs. Nontumor brain specimens were almost exclusively assigned to methylation class 3 (92%), which contained the lowest methylation scores. The primary GBMs were relatively unmethylated with respect to the 8 class 1 genes but more often contained hypermethylation of *HOXA9* and *SLIT2*. About 37% of primary GBMs fell into the class 2 methylation pattern that was driven by *HOXA9* and *SLIT2* methylation. Because *MAGEA1* and *PEG3* did not contribute significantly to the classification, they were not considered further.

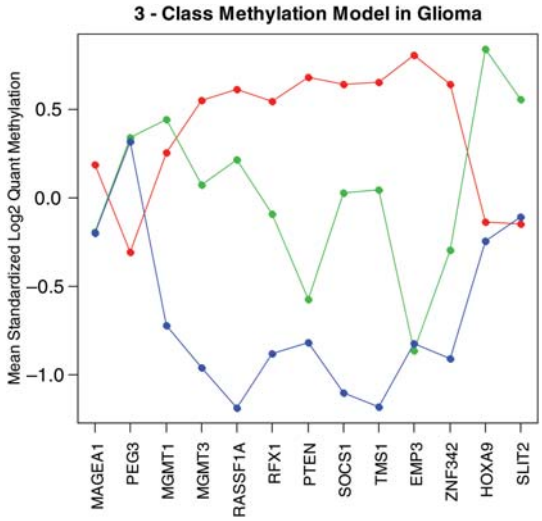

Fig. 1 Unsupervised clustering reveals 3 classes of DNA methylation in glioma. Quantitative methylation results for 3 methylation classes. The figure shows the difference in methylation level for each gene by methylation class. Methylation class 1: red, class 2: green, class 3: blue.

Table 2. Distribution of Methylation Classes 1, 2, and 3 by Histology

Histology/ Grade	N	Methylation Class					
		Class 1		Class 2		Class 3	
		N	Row %	N	Row %	N	Row %
Astrocytoma/II	28	18	64	5	18	5	18
Astrocytoma/III	9	7	78	1	11	1	11
Primary GBM	52	6	12	19	37	27	52
Secondary GBM	11	8	73	2	18	1	9
Oligo[a]/II and III	54	50	93	2	4	2	4
Nontumor brain	13	0	0	1	8	12	92
All	167	89	53	30	18	48	29

[a]Oligo includes oligodendroglioma and oligoastrocytoma.

Associations of Patient Characteristics with DNA Hypermethylation Profiles

The average ages at diagnosis for patients with the different subtypes of glioma were consistent with historical data.[3] As expected, patients with secondary GBM were about 10 years younger than those with primary GBM. Of interest among primary GBM patients were 6 cases with class 1 hypermethylation, which is associated with early age of diagnosis and gliomas of lower grade. Patients with primary GBM with class 1 methylation patterns were younger at diagnosis compared with other patients with primary GBM (mean 47 vs. 55 years old and median 37 vs. 53 years old for class 1 GBM and class 2 GBM, respectively).

Associations of EZH2 and IGFBP2 Expression with Glioma Histology and Methylation Class

EZH2 (total) and *IGFBP2* expression in relation to glioma subtypes and methylation patterns are summarized in Tables 3 and 4, respectively. *EZH2* was overexpressed in all grades of glioma but was greatest among GBMs. The genomic region containing *EZH2* was assessed for copy number changes in 60 tumors, including those containing the highest expression results. We found no evidence of *EZH2* amplification, as all RQ values were <1.5 for all tumors tested (data not shown). No significant correlations were noted between amplification of the epidermal growth factor receptor gene (*EGFR*) or *TP53* mutation and *EZH2* (data not shown). Consistent with previous studies, *IGFBP2* was highly expressed in GBM tumors (80%) and only rarely expressed in lower-grade astrocytic or oligodendroglial tumors (6%). Because *IGFBP2* overexpression is so infrequent among lower-grade tumors, we focused our analysis on primary GBMs to explore the associations of *IGFBP2* and *EZH2* expression with methylation class. When the mean methylation score for the 8 genes that define class 1 methylation were regressed against the expression values for *IGFBP2* and *EZH2*, *EZH2* positively associated with class 1

Table 3. Association of *EZH2* and *IGFBP2* Expression with Histological Subtype and Grade in Glioma

Histology/Grade	*EZH2* Expression[a]				*IGFBP2* Expression			
	N	Mean[b]	Standard Error	% Overexpressing[c]	N	Mean[b]	Standard Error	% Overexpressing[c]
Oligo[d]/II and III	15	3	0·6	73	18	0	0·1	6
Astrocytoma/II	15	3	0·8	53	15	1	0·7	7
Primary GBM	25	10	1·8	92	26	8	2·1	81
Secondary GBM	5	4	1·8	60	5	10	5·1	80
Total	60			75	64			42
	ANOVA p-value = 0·002				ANOVA p-value = 0·0018			

ANOVA, analysis of variance.
[a]Total transcripts of EZH2 are shown.
[b]Fold increase of relative quantification in glioma tumors compared with normal brain.
[c]Overexpressing tumors defined as having >1.5-fold expression compared with normal brain tissues.
[d]Oligo includes oligodendroglioma and oligoastrocytoma.
Two-sample *t*-tests comparing *EZH2* expression between the different histological groups found significant *p*-values of 0.0055 and 0.0097 between primary GBMs and oligos and primary GBMs and grade II astros, respectively.
Two-sample *t*-tests comparing *EZH2* expression between the different histological groups found significant *p*-values of 0.0037, 0.0013, 0.0144, and 0.0089 between primary GBMs and oligos, secondary GBMs and oligos, primary GBMs and grade II astros, and secondary GBMs and grade II astros, respectively.

Table 4. Association of *EZH2* and *IGFBP2* Expression with Methylation Classes in Glioma (all histologies)

Methylation Classes	*EZH2* Expression[a]				*IGFBP2* Expression			
	N	Mean[b]	StdErr	% Overexpressing[c]	N	Mean[b]	StdErr	% Overexpressing[c]
Class I	34	4	0·7	74	38	1	0·4	18
Class II	13	10	2·5	85	13	11	4	69
Class III	13	7	2·6	56	13	8	2·1	85
Total	60			75	64			42
	ANOVA p-value = 0·0601				ANOVA p-value = 0·0003			

ANOVA, analysis of variance.
[a]Total transcripts of *EZH2* are shown.
[b]Fold increase of relative quantification in glioma tumors compared with normal brain.
[c]Overexpressing tumors defined as having >1.5-fold expression compared with normal brain tissues.
Two-sample *t*-tests comparing *EZH2* expression between the methylation classes found a significant *p*-value of 0.0084 between class I and II.
Two-sample *t*-tests comparing *IGFBP2* expression between the methylation classes found significant *p*-values of 0.0002 and <0.0001 between class I and II and class I and III, respectively.

methylation, whereas *IGFBP2* was significantly inversely related to class 1 methylation among primary GBMs (Supplementary Material, Table S2). This result is graphically illustrated in Figure 2A and B. Those primary GBMs that fell into class 1 methylation clearly contain elevated *EZH2*, but in contrast to other GBMs demonstrated no or very low *IGFBP2* expression ($p < 0.008$).

Association of LINE1 Methylation with Methylation Class

To explore possible relationships between gene-specific and global DNA methylation, we compared the LINE1 methylation scores among different subtypes of glioma and according to their DNA methylation class, as determined using our 12-gene panel. The results (Fig. 3) indicate significant differences in LINE1 methylation among glioma subtypes ($p < 0.001$). Relatively greater LINE1 methylation was common among astrocytoma, oligodendroglioma, and oligoastrocytoma. GBM tumors demonstrated the greatest heterogeneity in LINE1 methylation and the lowest LINE1 scores (global hypomethylation) among the subtypes. LINE1 methylation was significantly higher among those gliomas classified as having a class 1 (hypermethylation) pattern of genic methylation. Thus, coordinate methylation of genes having the class 1 pattern of methylation is accompanied by higher levels of LINE1 methylation.

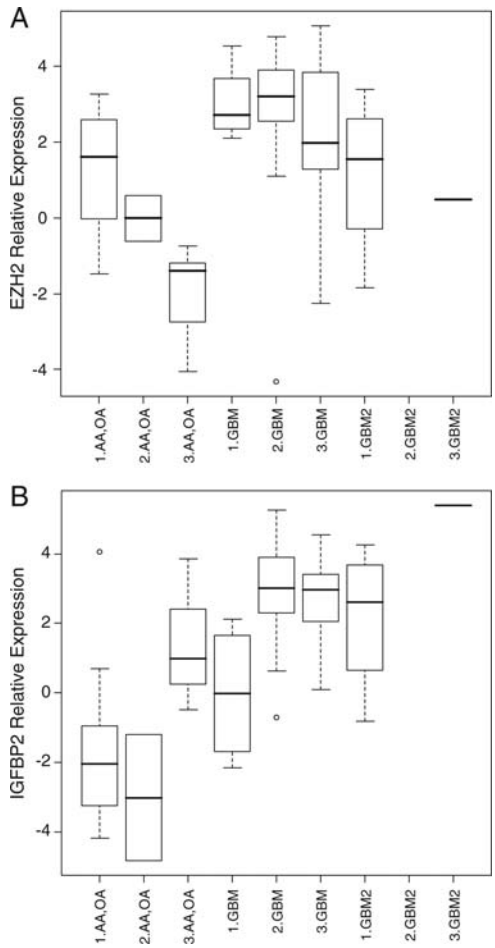

Fig. 2 Associations of EZH2 and IGFBP2 expression with DNA methylation classes. A. The figures shows the relative mRNA expression levels of EZH2 for lower grade glial tumors and GBMs, left and right panels, respectively. The EZH2 level corresponding to each methylation class is depicted within the two subtypes of glioma. When only one observation was made a single horizontal line appears. B. The figure shows the relative mRNA expression levels of IGBP2 for lower grade glial tumors and GBMs, left and right panels, respectively. The IGFBP2 level corresponding to each methylation class is depicted within the two subtypes of glioma. When only one observation was made a single horizontal line appears.

Association of Methylation Class with Patient Survival Time

The log rank test of Kaplan-Meier plots indicated a significant association of tumor methylation class with patient survival time ($p < 0.001$). The Cox multivariate analysis indicated that methylation class remained statistically significant when the model contained important predictors of patient outcome (Fig. 4). Class 1 pattern associated with hypermethylation of genes was associated with the longest survival times.

No Association of 1p/19q Deletion with Methylation Class

Ten tumors (4 oligoastrocytoma II and 6 oligodendroglioma II) had data on the 1p/19q deletion from Nimblegen array analysis of comparative genomic hybridization. All tumors, regardless of 1p/19q status, showed the class 1 hypermethylation pattern. Thus, 1p/19q deletion seems independent of DNA hypermethylation in this limited sample.

Discussion

Although distinct DNA hypermethylation patterns have been recognized for some time in human cancer, only recently have mechanisms emerged that might explain the targeting of specific groups of genes for aberrant methylation. The clear differentiation of secondary from primary GBM by methylation profiles confirmed our *a priori* hypothesis based on studies of individual genes and indicates the potential clinical value of methylation profiles in distinguishing the two types of GBM. A recent study proposed using *EMP3* methylation alone as a marker to differentiate secondary from primary GBM[6] (Supplementary Material, Table S3). In addition to *EMP3*, the present study identified 7 other genes differentially methylated in secondary and primary GBMs. Combining our results with those of earlier reports[7,8] could provide a highly discriminating panel for classifying these epigenetic subtypes of GBM (Supplementary Material, Table S3). In one case, both low- and high-grade glioma tissues were available, and we found that the class 1 pattern was retained in the

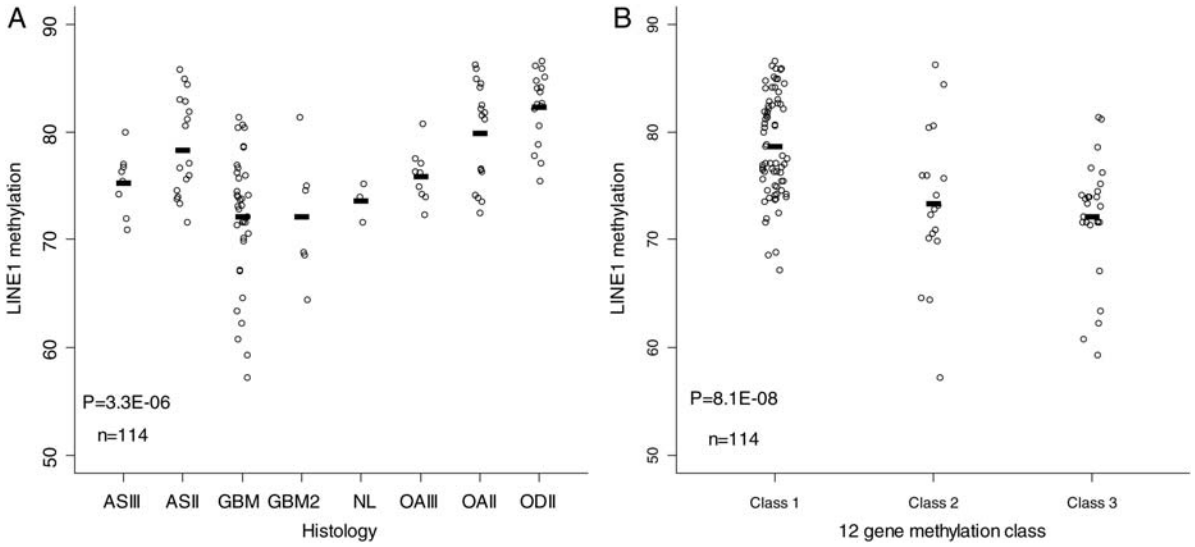

Fig. 3 LINE1 DNA methylation values. Panel A shows mean LINE1 scores stratified by histopathologic subtype; NL indicates non-malignant brain tissues. Panel B shows mean LINE1 scores stratified by methylation class.

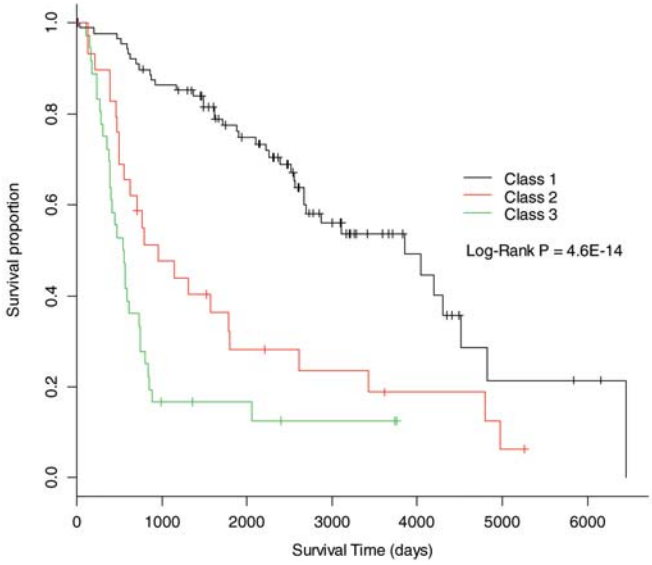

Covariate	HR	95% CI	*P*
Age	1.0	1.0 - 1.1	1.50E-04
Gender			
Female	1.0	Referent	-
Male	0.8	0.53 - 1.3	0.35
Grade			
2	1.0	Referent	-
3	0.9	0.53 - 1.3	0.72
4	7.0	3.8 - 13.1	7.6E-10
Methylation Class			
Class 1	1.0	Referent	-
Class 2	1.2	0.71 - 2.2	0.45
Class 3	2.5	1.4 - 4.7	< 0.003

n=154

Fig. 4 Survival analysis among glioma cases by DNA methylation class. The picture (left) shows Kaplan-Meier survival strata for methylation classes where hash marks are censored values. The table (right) shows the Cox proportional hazards model of survival modeling DNA methylation classes and covariates.

high-grade lesion. Another potential application of such an approach is suggested by our results in primary GBM in which 12% of cases displayed a methylation profile highly similar to known secondary GBMs that progressed from lower-grade tumors. Younger aged primary GBM cases were overrepresented in this group, and we speculate that they may represent a distinct epigenetic subtype that arises from clinically unrecognized lower-grade lesions. Epidemiologic studies have suggested the existence of long-latency, high-grade glioma based on the significantly higher incidence of seizure disorders preceding GBM diagnosis by 8–11 years.[59] Molecular features such as mutations of TP53 and amplification of EGFR suggest that younger aged primary GBM comprises different genetic subtypes,[2] but the distinctions noted here based on methylation profile provide an even more robust segregation.

Our 12-gene panel contained two genes, *HOXA9* and *SLIT2*, that are recognized as PRC targets in embryonic stem cells, whereas the others are not known targets. A significant result of our study is that glioma tumor types were segregated by DNA methylation profile according to the PRC target status of hypermethylated genes. The clustering of gene methylation in 37% of primary GBMs was driven by the hypermethylation of PRC targets *HOXA9* and *SLIT2*, whereas the coordinate methylation of 8 non-PRC targets characterized secondary GBMs and astrocytoma stage II, anaplastic astrocytoma III, oligodendroglioma II, and oligoastroglioma II.

An additional aim of this study was to characterize patterns of aberrant DNA methylation in glioma and explore the potential roles of PRC and PI3K/Akt in these events by assessing the overexpression of *EZH2* and *IGFBP2* mRNA, respectively. We assessed *EZH2* in primary glioma of different grades and found that *EZH2* was overexpressed in most astrocytic and oligodendroglial tumors, but even more highly expressed in the higher-grade GBM tumors. Thus, our results follow the trend seen in other cancer types of increasing PRC pathway activation and aggressive tumor characteristics. We assessed three different qRT-PCR methods for *EZH2* mRNA expression and found that both the short and long *EZH2* isoforms showed very similar associations with methylation class (data not shown).The long *EZH2* isoform was the predominant form in glioma, as has been reported previously in normal tissues.[60] Previous studies postulated that gene amplification may be a mechanism for the induction of *EZH2* in non-glial tumors.[32] We found no evidence of increased *EZH2* gene copy number in our study, which makes amplification an unlikely mechanism for *EZH2* overexpression in glioma.

IGFBP2, like *EZH2*, was highly overexpressed in GBM but in contrast to *EZH2* was not detectable among lower-grade astrocytic and oligodendroglial tumors (with the exception of two grade III astrocytomas). However, *IGFBP2* levels varied considerably within primary GBMs, and lower *IGFBP2* levels were observed among tumors with a distinct methylation profile and earlier age at onset. Primary GBMs without *IGFBP2* overexpression exhibited a phenotype defined by methylation of 8 non-PRC targets. In contrast, PRC targets *HOXA9* and *SLIT2* were methylated in GBMs containing both *IGFBP2* and *EZH2* overexpression. Although our observation that *IGFBP2* expression is associated with DNA methylation phenotype is novel, our study does not provide evidence that this relationship is causal with respect to PI3K/Akt. Nonetheless, any connection between *IGFBP2* expression and PI3K/Akt pathway activation rests on the validity of *IGFBP2* as a marker of this pathway. Several studies support this assumption[42–45]; however, there may be other phenomena such as tissue hypoxia[61] that could be associated with both *IGFBP2* expression and DNA methylation. Furthermore, our hypothesis that Akt activation could indirectly affect DNA methylation by phosphorylating EZH2[41] must be regarded as speculative, although the proposed pivotal role of H3K27me3 and EZH2 in controlling methylation provides a strong rationale for future studies to explore DNA methylation in cells with and without Akt activation. A recent study[62] questioned the proposal that H3K27me3 is universally linked with DNA hypermethylation of PRC gene targets. The convergence of H3K27me3 with DNA methylation mechanisms was posited to be dependent on cell type.[62] Our study provides a clue that PRC targeting for methylation may be modified by the activation status of the PI3K/Akt pathway. Supporting this idea further is our observation that a GBM progressing from an earlier astrocytoma II retained its class I methylation and low PRC target methylation and that both first tumor and second tumor were negative for IGFBP2 expression.

The finding that a pattern of gene hypermethylation correlated with LINE1 methylation indicates that a generalized mechanism operates in some subtypes of glioma, acting on specific genes associated with CpG sites as well as nongenic repetitive DNA regions. In addition, this evidence of epigenetic dysregulation was strongly linked with patient survival and low expression of the IGFBP2 gene. Taken together, these studies suggest a convergence of pathways that may offer new approaches for improving patient prognostication and therapeutic targets.

Our study has some notable strengths and limitations. One strength is our application of a quantitative MS-PCR method that has been shown to be superior to conventional MS-PCR for detecting hypermethylation patterns in human tumors. We also applied a novel unsupervised clustering methodology to create methylation classes that has advantages over conventional methods.[58] A limitation of our work is the relatively small number of genes examined, which prevents us from knowing how generalizable our findings might be regarding PRC target and non–target gene methylation in different types of glioma. Future studies that expand the set of target genes interrogated will further inform PRC target versus nontarget methylation in these diseases. Our findings provide new insights into the associations of DNA hypermethylation profiles with 2 expression biomarkers that have strong connections to tumor progression and cancer survival.

Conflict of interest statement. None declared.

Supplementary Material

Supplementary material is available at *Neuro-Oncology* journal online.

Funding

Grant support: ES06717, NCI CA126831; p50CA0927257.

References

1. Louis DN, Ohgaki H, Wiestler OD, et al. The 2007 WHO classification of tumours of the central nervous system. *Acta Neuropathol (Berl).* 2007;114(2):97–109.

2. Wiencke JK, Aldape K, McMillan A, et al. Molecular features of adult glioma associated with patient race/ethnicity, age, and a polymorphism in O6-methylguanine-DNA-methyltransferase. *Cancer Epidemiol Biomarkers Prev.* 2005;14(7):1774–1783.

3. Ohgaki H, Kleihues P. Genetic pathways to primary and secondary glioblastoma. *Am J Pathol.* 2007;170(5):1445–1453.
4. Furnari FB, Fenton T, Bachoo RM, et al. Malignant astrocytic glioma: genetics, biology, and paths to treatment. *Genes Dev.* 2007;21(21):2683–2710.
5. Jones PA, Baylin SB. The epigenomics of cancer. *Cell.* 2007;128(4):683–692.
6. Kunitz A, Wolter M, van den Boom J, et al. DNA hypermethylation and aberrant expression of the EMP3 gene at 19q13.3 in human gliomas. *Brain Pathol.* 2007;17(4):363–370.
7. Nakamura M, Ishida E, Shimada K, et al. Frequent LOH on 22q12.3 and TIMP-3 inactivation occur in the progression to secondary glioblastomas. *Lab Invest.* 2005;85(2):165–175.
8. Nakamura M, Watanabe T, Yonekawa Y, Kleihues P, Ohgaki H. Promoter methylation of the DNA repair gene MGMT in astrocytomas is frequently associated with G:C –> A:T mutations of the TP53 tumor suppressor gene. *Carcinogenesis.* 2001;22(10):1715–1719.
9. Nakamura M, Yonekawa Y, Kleihues P, Ohgaki H. Promoter hypermethylation of the RB1 gene in glioblastomas. *Lab Invest.* 2001;81(1):77–82.
10. Wiencke JK, Zheng S, Jelluma N, et al. Methylation of the PTEN promoter defines low-grade gliomas and secondary glioblastoma. *Neuro Oncol.* 2007;9(3):271–279.
11. Costello JF, Plass C, Cavenee WK. Aberrant methylation of genes in low-grade astrocytomas. *Brain Tumor Pathol.* 2000;17(2):49–56.
12. Dong SM, Pang JC, Poon WS, et al. Concurrent hypermethylation of multiple genes is associated with grade of oligodendroglial tumors. *J Neuropathol Exp Neurol.* 2001;60(8):808–816.
13. Uhlmann K, Rohde K, Zeller C, et al. Distinct methylation profiles of glioma subtypes. *Int J Cancer.* 2003;106(1):52–59.
14. Weller M, Stupp R, Reifenberger G, et al. MGMT promoter methylation in malignant gliomas: ready for personalized medicine? *Nat Rev Neurol.* 2010;6(1):39–51.
15. Michalowski MB, de Fraipont F, Michelland S, et al. Methylation of RASSF1A and TRAIL pathway-related genes is frequent in childhood intracranial ependymomas and benign choroid plexus papilloma. *Cancer Genet Cytogenet.* 2006;166(1):74–81.
16. Ohashi Y, Ueda M, Kawase T, Kawakami Y, Toda M. Identification of an epigenetically silenced gene, RFX1, in human glioma cells using restriction landmark genomic scanning. *Oncogene.* 2004;23(47):7772–7779.
17. Alaminos M, Davalos V, Ropero S, et al. EMP3, a myelin-related gene located in the critical 19q13.3 region, is epigenetically silenced and exhibits features of a candidate tumor suppressor in glioma and neuroblastoma. *Cancer Res.* 2005;65(7):2565–2571.
18. Stone AR, Bobo W, Brat DJ, Devi NS, Van Meir EG, Vertino PM. Aberrant methylation and down-regulation of TMS1/ASC in human glioblastoma. *Am J Pathol.* 2004;165(4):1151–1161.
19. Hong C, Bollen AW, Costello JF. The contribution of genetic and epigenetic mechanisms to gene silencing in oligodendrogliomas. *Cancer Res.* 2003;63(22):7600–7605.
20. Martini M, Pallini R, Luongo G, Cenci T, Lucantoni C, Larocca LM. Prognostic relevance of SOCS3 hypermethylation in patients with glioblastoma multiforme. *Int J Cancer.* 2008;123(12):2955–2960.
21. Maegawa S, Yoshioka H, Itaba N, et al. Epigenetic silencing of PEG3 gene expression in human glioma cell lines. *Mol Carcinog.* 2001;31(1):1–9.
22. Yu J, Zhang H, Gu J, et al. Methylation profiles of thirty four promoter-CpG islands and concordant methylation behaviours of sixteen genes that may contribute to carcinogenesis of astrocytoma. *BMC Cancer.* 2004;4(1):65.
23. Alaminos M, Davalos V, Cheung NK, Gerald WL, Esteller M. Clustering of gene hypermethylation associated with clinical risk groups in neuroblastoma. *J Natl Cancer Inst.* 2004;96(16):1208–1219.
24. Dallol A, Krex D, Hesson L, Eng C, Maher ER, Latif F. Frequent epigenetic inactivation of the SLIT2 gene in gliomas. *Oncogene.* 2003;22(29):4611–4616.
25. Ohm JE, McGarvey KM, Yu X, et al. A stem cell-like chromatin pattern may predispose tumor suppressor genes to DNA hypermethylation and heritable silencing. *Nat Genet.* 2007;39(2):237–242.
26. Rajasekhar VK, Dalerba P, Passegue E, Lagasse E, Najbauer J. Stem cells, cancer, and context dependence. *Stem Cells.* 2007;26:292–298.
27. Vire E, Brenner C, Deplus R, et al. The Polycomb group protein EZH2 directly controls DNA methylation. *Nature.* 2006;439(7078):871–874.
28. Keshet I, Schlesinger Y, Farkash S, et al. Evidence for an instructive mechanism of de novo methylation in cancer cells. *Nat Genet.* 2006;38(2):149–153.
29. Ohm JE, Baylin SB. Stem cell chromatin patterns: an instructive mechanism for DNA hypermethylation? *Cell Cycle.* 2007;6(9):1040–1043.
30. Schlesinger Y, Straussman R, Keshet I, et al. Polycomb-mediated methylation on Lys27 of histone H3 pre-marks genes for de novo methylation in cancer. *Nat Genet.* 2007;39(2):232–236.
31. Bachmann N, Hoegel J, Haeusler J, et al. Mutation screen and association study of EZH2 as a susceptibility gene for aggressive prostate cancer. *Prostate.* 2005;65(3):252–259.
32. Berezovska OP, Glinskii AB, Yang Z, Li XM, Hoffman RM, Glinsky GV. Essential role for activation of the Polycomb group (PcG) protein chromatin silencing pathway in metastatic prostate cancer. *Cell Cycle.* 2006;5(16):1886–1901.
33. Collett K, Eide GE, Arnes J, et al. Expression of enhancer of zeste homologue 2 is significantly associated with increased tumor cell proliferation and is a marker of aggressive breast cancer. *Clin Cancer Res.* 2006;12(4):1168–1174.
34. Raman JD, Mongan NP, Tickoo SK, Boorjian SA, Scherr DS, Gudas LJ. Increased expression of the polycomb group gene, EZH2, in transitional cell carcinoma of the bladder. *Clin Cancer Res.* 2005;11(24 Pt 1):8570–8576.
35. van Leenders GJ, Dukers D, Hessels D, et al. Polycomb-group oncogenes EZH2, BMI1, and RING1 are overexpressed in prostate cancer with adverse pathologic and clinical features. *Eur Urol.* 2007;52(2):455–463.
36. Varambally S, Dhanasekaran SM, Zhou M, et al. The polycomb group protein EZH2 is involved in progression of prostate cancer. *Nature.* 2002;419(6907):624–629.
37. Weikert S, Christoph F, Kollermann J, et al. Expression levels of the EZH2 polycomb transcriptional repressor correlate with aggressiveness and invasive potential of bladder carcinomas. *Int J Mol Med.* 2005;16(2):349–353.
38. Yu J, Rhodes DR, Tomlins SA, et al. A polycomb repression signature in metastatic prostate cancer predicts cancer outcome. *Cancer Res.* 2007;67(22):10657–10663.
39. Hinz S, Kempkensteffen C, Weikert S, et al. EZH2 polycomb transcriptional repressor expression correlates with methylation of the APAF-1 gene in superficial transitional cell carcinoma of the bladder. *Tumour Biol.* 2007;28(3):151–157.

40. Beke L, Nuytten M, Van Eynde A, Beullens M, Bollen M. The gene encoding the prostatic tumor suppressor PSP94 is a target for repression by the Polycomb group protein EZH2. *Oncogene.* 2007;26(31):4590–4595.
41. Cha TL, Zhou BP, Xia W, et al. Akt-mediated phosphorylation of EZH2 suppresses methylation of lysine 27 in histone H3. *Science.* 2005;310(5746):306–310.
42. Levitt RJ, Georgescu MM, Pollak M. PTEN-induction in U251 glioma cells decreases the expression of insulin-like growth factor binding protein-2. *Biochem Biophys Res Commun.* 2005;336(4):1056–1061.
43. Mehrian-Shai R, Chen CD, Shi T, et al. Insulin growth factor-binding protein 2 is a candidate biomarker for PTEN status and PI3K/Akt pathway activation in glioblastoma and prostate cancer. *Proc Natl Acad Sci U S A.* 2007;104(13):5563–5568.
44. Dunlap SM, Celestino J, Wang H, et al. Insulin-like growth factor binding protein 2 promotes glioma development and progression. *Proc Natl Acad Sci U S A.* 2007;104(28):11736–11741.
45. Jiang R, Mircean C, Shmulevich I, et al. Pathway alterations during glioma progression revealed by reverse phase protein lysate arrays. *Proteomics.* 2006;6(10):2964–2971.
46. McDonald KL, O'Sullivan MG, Parkinson JF, et al. IQGAP1 and IGFBP2: valuable biomarkers for determining prognosis in glioma patients. *J Neuropathol Exp Neurol.* 2007;66(5):405–417.
47. Fuller GN, Hess KR, Rhee CH, et al. Molecular classification of human diffuse gliomas by multidimensional scaling analysis of gene expression profiles parallels morphology-based classification, correlates with survival, and reveals clinically-relevant novel glioma subsets. *Brain Pathol.* 2002;12(1):108–116.
48. Fuller GN, Rhee CH, Hess KR, et al. Reactivation of insulin-like growth factor binding protein 2 expression in glioblastoma multiforme: a revelation by parallel gene expression profiling. *Cancer Res.* 1999;59(17):4228–4232.
49. Godard S, Getz G, Delorenzi M, et al. Classification of human astrocytic gliomas on the basis of gene expression: a correlated group of genes with angiogenic activity emerges as a strong predictor of subtypes. *Cancer Res.* 2003;63(20):6613–6625.
50. Rickman DS, Bobek MP, Misek DE, et al. Distinctive molecular profiles of high-grade and low-grade gliomas based on oligonucleotide microarray analysis. *Cancer Res.* 2001;61(18):6885–6891.
51. Sallinen SL, Sallinen PK, Haapasalo HK, et al. Identification of differentially expressed genes in human gliomas by DNA microarray and tissue chip techniques. *Cancer Res.* 2000;60(23):6617–6622.
52. van Hattem WA, Carvalho R, Li A, Offerhaus GJ, Goggins M. Amplification of EMSY Gene in a Subset of Sporadic Pancreatic Adenocarcinomas. *Int J Clin Exp Pathol.* 2008;1(4):343–351.
53. Depreter M, Vandesompele J, Espeel M, Speleman F, Roels F. Modulation of the peroxisomal gene expression pattern by dehydroepiandrosterone and vitamin D: therapeutic implications. *J Endocrinol.* 2002;175(3):779–792.
54. Wilhelm CS, Kelsey KT, Butler R, et al. Implications of LINE1 methylation for bladder cancer risk in women. *Clin Cancer Res.* 2010;6(5):1682–1689.
55. Banfield JD, Raftery AE. Model-based Gaussian and non-Gaussian clustering. *Biometrics.* 1993;49:803–821.
56. Fraga MF, Esteller M. DNA methylation: a profile of methods and applications. *Biotechniques.* 2002;33(3):632, 634, 636–649.
57. Fraley C, Raftery AE. Enhanced Software for model-based clustering, discriminant analysis, and density estimation:MCLUST. *Journal of Classification.* 2003;20:263–286.
58. Houseman EA, Christensen BC, Yeh RF, et al. Model-based clustering of DNA methylation array data: a recursive-partitioning algorithm for high-dimensional data arising as a mixture of beta distributions. *BMC Bioinformatics.* 2008;9:365.
59. Schwartzbaum J, Jonsson F, Ahlbom A, et al. Prior hospitalization for epilepsy, diabetes, and stroke and subsequent glioma and meningioma risk. *Cancer Epidemiol Biomarkers Prev.* 2005;14(3):643–650.
60. Hobert O, Jallal B, Ullrich A. Interaction of Vav with ENX-1, a putative transcriptional regulator of homeobox gene expression. *Mol Cell Biol.* 1996;16(6):3066–3073.
61. Shahrzad S, Bertrand K, Minhas K, Coomber BL. Induction of DNA hypomethylation by tumor hypoxia. *Epigenetics.* 2007;2(2):119–125.
62. Kondo Y, Shen L, Cheng AS, et al. Gene silencing in cancer by histone H3 lysine 27 trimethylation independent of promoter DNA methylation. *Nat Genet.* 2008;40(6):741–750.